INVESTIGATION OF THE PHASE BIAS IN THE SHORT TERM INTERFEROGRAMS

Yasser Maghsoudi (1), Milan Lazecky (1), Homa Ansari (2), Andrew J. Hooper (1), Tim J. Wright (1)

(1) Center for the Observation and Modelling of Earthquakes,Volcanoes & Tectonics, (COMET), Institute of Geophysics and Tectonics, School of Earth and Environment, University of Leeds, LS2 9JT, UK
(2) Remote Sensing Technology Institute (IMF), German Aerospace Center (DLR)

IGARSS 2021 - 2021 IEEE International Geoscience and Remote Sensing Symposium | 978-1-6654-0369-6/21/$31.00 ©2021 IEEE | DOI: 10.1109/IGARSS47720.2021.9553631

ABSTRACT

Interferometric Synthetic Aperture Radar (InSAR) is a powerful tool for monitoring ground deformation associated with earthquakes, volcanoes, landslides, and different anthropogenic activities. The accuracy of the estimated deformation depends on a number of parameters including tropospheric and ionospheric delays, unwrapping errors, phase decorrelation due to changes in scattering behavior and system noise. However, recently an additional source of phase noise has been identified [1], which is strongest in short-interval multi-looked interferograms and, unlike other sources of noise, leads to biased, non-zero loop closure phases. This is problematic for time-series analysis because short-interval interferograms may be the only ones that maintain coherence for some areas. In this study, we explore the characteristics of this phenomenon and propose a mitigation strategy.

Index Terms— InSAR, phase bias, velocity

1. INTRODUCTION

If φ_{ij}, φ_{jk} and φ_{ik} are three averaged interferometric phases obtained from three acquisitions i, j and k, in the absence of the phase inconsistency, the expected value of the sum will be zero. However, due to the lack of consistency, this is not always the case. It was observed in previous studies that changes in soil moisture and in the water content of vegetation may lead to such phase inconsistencies [2-3].

Even though the amount of the phase bias is not significant in each individual interferogram, its accumulation through the time can highly affect the final estimated deformation.

For the mitigations strategies, we can either correct the interferograms using the estimated moisture-induced phase [3] or the phase linking approaches such as [1,4] could be adopted.

The main objectives of this research is to explore the characteristics of this phase bias by investigating the temporal and spatial behavior of the phase bias. Then, we provide an empirical strategy to deal with this phenomenon.

We chose a study area in the west of Turkey, which is regularly monitored by Sentinel-1 A and B. In this study, we processed a one year data from track 36 spanning February 2017 to February 2018. In this study, for each epoch, we generated three interferograms using the follow-up 6, 12 and 18-day acquisitions. All the generated interferograms are multilooked by factors of 5 in the range and 20 in the azimuth directions. The land cover is heterogeneous which allows investigating the bias effect in different land covers ranging from more coherent urban areas to the agricultural and forest areas.

2. PHASE BIAS CHARACTERIZATION

To isolate the phase bias, we construct "daisy chain" sums of interferograms covering an identical 360 day time period, but using different time period interferograms (6,12,18, 24...180 days). Conventional noise sources in each of these sums should be nearly identical, and any differences should be small and centred on zero. However, we find that the daisy-chain sums that use short-time-interval interferograms are biased for some pixels, and that the bias appears to be spatially correlated. The bias is much weaker in longer-interval daisy-chain sums.

In Fig. 1, the n day refers to the interferogram with the n day temporal baseline. The (60 day – 6 day), for example, shows the difference between a 60-day interferogram from the summation of 6-day interferograms spanning the same time. Assuming that the long interferograms (e.g. 60-day here) are minimally affected by the bias, Fig. 1 shows how the shorter interferograms are more affected by this phenomenon.

Authorized licensed use limited to: Deutsches Zentrum fuer Luft- und Raumfahrt. Downloaded on November 23,2022 at 21:16:54 UTC from IEEE Xplore. Restrictions apply.

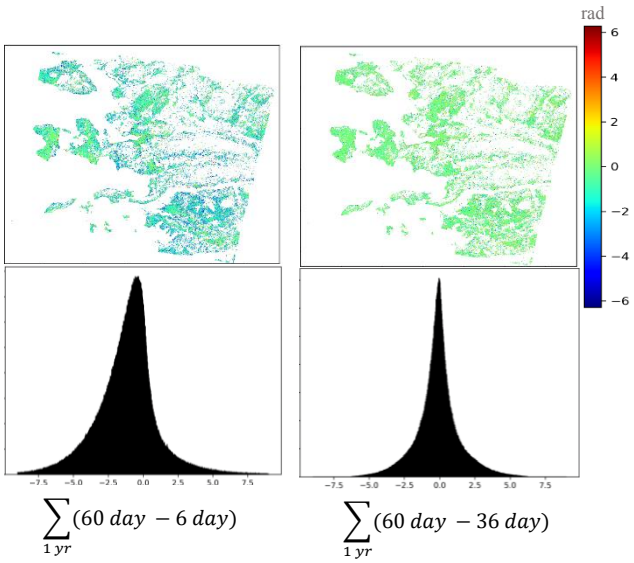

Fig. 1. The difference between the 60-day interferograms and the corresponding 6-day interferograms (left) and the 60-day interferograms and the corresponding 36-day interferograms (right).

3. PHASE BIAS CORRECTION

In this study, we aim at correcting all the short term 6, 12 and 18-day interferograms using an empirical method. Considering an unknown bias term for each interferogram would eventually end up in an under-determined system. To avoid this, we assume that the bias in interferograms is linearly related to sum of biases in shorter interferograms spanning the same time. We employed this assumption as a basis for the estimation of the bias in each interferogram. Considering $\delta_{i,j}$ as the bias in the interferogram between image *i* and *j*, the two assumptions are given by:

$$\delta_{i,i+2} = a_1\ (\delta_{i,i+1} + \delta_{i+1,i+2}) \qquad (1)$$

$$\delta_{i,i+3} = a_2(\delta_{i,i+1} + \delta_{i+1,i+2} + \delta_{i+2,i+3})$$

in which a_1 and a_2 are the constant values which linearly relate the longer interferogram bias to sum of the corresponding biases in the short interferograms. In this study, we estimated the parameters a_1 and a_2 using:

$$a_1 = \frac{\sum_{1\,yr}(360\ day\ -12\ day)}{\sum_{1\,yr}(360\ day\ -6\ day)} \qquad (2)$$

$$a_2 = \frac{\sum_{1\,yr}(360\ day\ -18\ day)}{\sum_{1\,yr}(360\ day\ -6\ day)}$$

Plugging the calculated parameters a_1 and a_2 into Eq. 1, and by exploiting all the generated interferograms, a set of linear equations are formed. The unknown bias values are then estimated using a least square inversion. Upon the estimation of the bias terms, every single interferogram will be corrected.

4. VELOCITIES

Fig. 2 shows how the 1 year cumulative residuals obtained by $\sum_{1\,yr}(18\ day\ -6\ day)$ are reduced after correcting the interferograms for the biases.

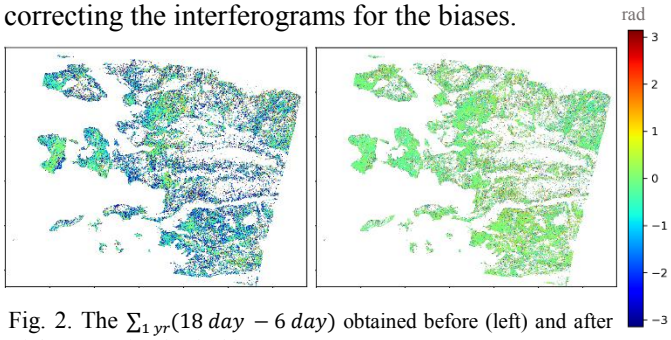

Fig. 2. The $\sum_{1\,yr}(18\ day\ -6\ day)$ obtained before (left) and after (right) correcting for the bias.

In the next experiment, the velocities were obtained using SBAS inversion strategy before and after correcting for the bias terms. We used the CAESAR phase linking approach [4] as our reference method. It should be noted that the CAESAR algorithm is based on the eigen-decomposition of the full coherency matrix. Fig. 3 shows the difference between the CAESAR estimated velocity and the velocity obtained by the SBAS method before and after bias correction. It is evident from Fig. 3 that correcting for the phase bias has provided a more similar results to the CAESAR approach. For a better visualization, two subsets are selected in Fig. 3 and are illustrated in Fig 4.

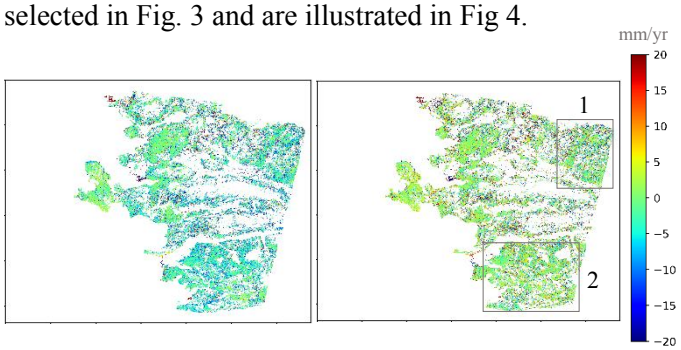

Fig. 3. The difference between the CAESAR velocity and the velocity estimated by SBAS before (left) and after (right) bias correction

Authorized licensed use limited to: Deutsches Zentrum fuer Luft- und Raumfahrt. Downloaded on November 23,2022 at 21:16:54 UTC from IEEE Xplore. Restrictions apply.

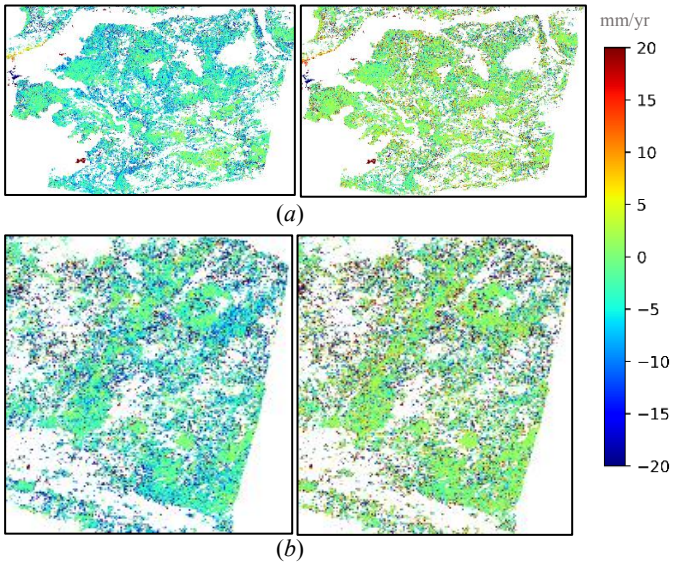

Fig. 4. The differences between the CAESAR velocity and the velocity estimated by SBAS before (left) and after (right) bias correction for the subset 1 (*a*) and subset 2 (*b*).

5. EVALUATION OF PHYSICAL SOURCES

The fading InSAR signal is reportedly (partly) induced by physical sources such as response of vegetation and soil moisture variation [2,3]. We have performed a correlation analysis evaluating several meteorologic variables as the potential sources of the phase bias of short B_{temp} interferograms. We have indicated two potential sources having relatively high correlation slopes in both interferometric phase difference and/or residuals of the interferomertic triplet loop closure: soil moisture and (cummulated) temperature.

For our correlation with soil moisture variation, we have used data calculated from the amplitude of corresponding Sentinel-1 acquisitions [5]. We will update this paragraph with a clear example.

We have used ECMWF ERA5 model to acquire daily amplitude of temperature and calculated Growing Degree Day (GDD) index corresponding to our dataset, as an acummulation of average daily temperature since the first acquisition date, minus plant type dependent base temperature T_{base}. We have chosen T_{base} = 10 K and zeroed lower GDD values in order to limit the measure to seasons of vegetation growth (NB: the physical meaning of GDD correlation would include soil moisture variation due to decreased temperature during rain periods). The selected area of interest is an agricultural area where the uncorrected fading signal causes significant bias in the time series (see Fig. 5).

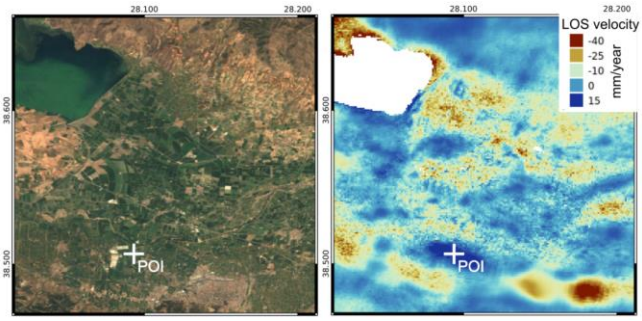

Fig. 5. Selected region of interest and its original LiCSBAS-based LOS velocity output.

Phase of differential interferograms within B_{temp}=(6,12,18) days correlate with differential values of corresponding GDD (dGDD). Fig. 5 and 6 visualize location of a point of interest (POI) having strong negative correlation coefficient of approx. -0.3 in all Btemp cases, and a relatively high estimate of LOS velocity of ~13 mm/year.

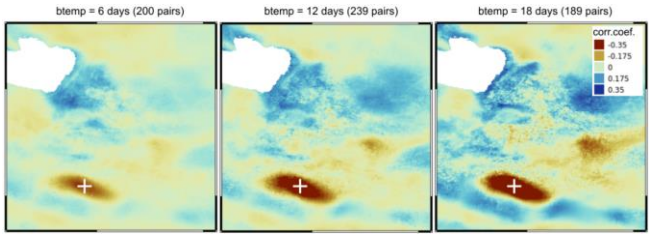

Fig. 6. Pearson correlation coefficient between dGDD values and unwrapped interferograms having Btemp = 6, 12 or 18 days.

We were studying the loop closure phase residuals within short B_{temp} combinations - point POI shows a positive correlation of approx. 0.3 between the loop closure residuals and dGDD for the time period within triplets of 6+6-12 days interferograms and 6+6+6-18 quadruplets. The annual view on both wrapped triplet/quadruplet residuals and scaled variation of dGDD values is shown in Fig. 7. More cumulated 6-days bias in the case of 6+6+6-18 quadruplets show possibly agriculture-related signal having large variation in spring season while keeping consistent annual period, similar to dGDD distribution.

Authorized licensed use limited to: Deutsches Zentrum fuer Luft- und Raumfahrt. Downloaded on November 23,2022 at 21:16:54 UTC from IEEE Xplore. Restrictions apply.

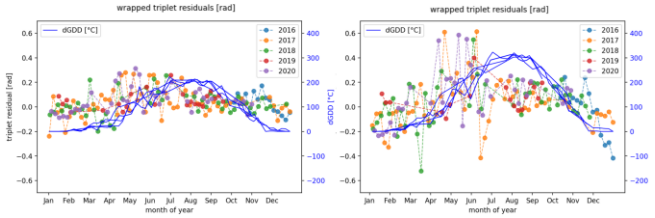

Fig. 7. Annual distribution of wrapped loop closure phase residuals of (left) triplets of combination of 6+6-12 days interferograms and (right) quadruplets of combination of 6+6+6-18 days interferograms, overlaid by a scaled distribution of corresponding dGDD values.

6. REFERENCES

[1] H. Ansari, F. De Zan and A. Parizzi, "Study of Systematic Bias in Measuring Surface Deformation With SAR Interferometry," *IEEE Transactions on Geoscience and Remote Sensing*, doi: 10.1109/TGRS.2020.3003421.

[2] F. De Zan, A. Parizzi, P. Prats-Iraola, and P. López-Dekker, "A SAR interferometric model for soil moisture," IEEE Transactions on Geoscience and Remote Sensing, vol. 52, no. 1, pp. 418–425, Jan. 2014.

[3] F. De Zan and G. Gomba, "Vegetation and soil moisture inversion from SAR closure phases: First experiments and results," Remote Sensing of Environment, vol. 217, pp. 562–572, Nov. 2018.

[4] G. Fornaro, S. Verde, D. Reale, and A. Pauciullo, "CAESAR: An approach based on covariance matrix decomposition to improve multibaseline–multitemporal interferometric SAR processing," IEEE Transactions on Geoscience and Remote Sensing, vol. 53, no. 4, pp. 2050–2065, Apr. 2015.

[5] A. Gruber, W. Wagner, A. Hegyiová, F. Greifeneder and S. Schlaffer, "Potential of Sentinel-1 for high-resolution soil moisture monitoring," 2013 IEEE International Geoscience and Remote Sensing Symposium - IGARSS, Melbourne, VIC, 2013, pp. 4030-4033, doi: 10.1109/IGARSS.2013.6723717

Authorized licensed use limited to: Deutsches Zentrum fuer Luft- und Raumfahrt. Downloaded on November 23,2022 at 21:16:54 UTC from IEEE Xplore. Restrictions apply.